

## EFFECTS OF 10 MEV PROTON IRRADIATION OF III-V SOLAR CELLS

E. Yaccuzzi<sup>1,2</sup>, M. Ochoa<sup>3</sup>, M. Barrera<sup>1,2</sup>, E. Barrigón<sup>3</sup>, S. Rodríguez<sup>1</sup>, P. Espinet<sup>3</sup>, M.L. Ibarra<sup>1,2</sup>, J. García<sup>1,2</sup>, E.M. Godfrin<sup>1</sup>, M. Alurralde<sup>1</sup>, F. Rubinelli<sup>4</sup>, C. Algora<sup>3</sup>, I. Rey-Stolle<sup>3</sup>, J. Plá<sup>1,2</sup>

<sup>1</sup> Departamento Energía Solar - Gerencia Investigación y Aplicaciones - CNEA

<sup>2</sup> Consejo Nacional de Investigaciones Científicas y Técnicas (CONICET)

Av. General Paz 1499 - (1650) San Martín - Argentina

Tel. (+54-11) 6772-7128, Fax (+54-11) 6772-7121, jpla@tandar.cnea.gov.ar

<sup>3</sup>Instituto de Energía Solar - Universidad Politécnica de Madrid

Av. Complutense 30; 28040 Madrid -Spain

<sup>4</sup>INTEC-CONICET, Universidad Nacional del Litoral

Güemes 3450, 3000 Santa Fe - Argentina

**ABSTRACT:** In this work we present our latest results and analysis of a 10 MeV proton irradiation experiment performed on III-V solar cells. A set of representative devices were irradiated for different fluences, including lattice-matched GaInP/GaInAs/Ge triple junction, GaInP/Ge double junction, and GaAs and Ge single junction solar cells. The methodology applied included the irradiation of two devices of each type; for a better control of the measurements, non-irradiated devices with the same characteristics of those irradiated were used as reference. The devices were monitored before and after each exposure by in-situ characterization of the electrical response under dark and under illumination using a solar simulator connected to the irradiation chamber through a borosilicate glass window. Ex-situ characterization techniques included dark and 1 sun AM0 illumination I-V curve and external quantum efficiency measurements. Furthermore, results of the numerical simulation of devices with D-AMPS-1D code are presented in order to give a physical interpretation of the results. DLTS spectroscopy preliminary results for single junction GaAs cells are also presented.

**Keywords:** Radiation Damage, III-V Semiconductors, Space Cells, Concentrator Cells

## 1 INTRODUCTION

Solar cells are the primary source of electrical power for spacecraft, satellites and other space vehicles. The devices in orbit suffer the irradiation of energetic charged particles, leading to degradation in their electrical and electronic properties.

The Solar Energy Department (DES) of the Argentine Atomic Energy Commission (CNEA) and the Institute of Solar Energy (IES) of the Technical University of Madrid (UPM), Spain, collaborate in a scientific project devoted to the study of III-V semiconductor-based solar cells. Both groups take advantage of their complementary expertise to study radiation damage on concentrating photovoltaic solar cells optimized for terrestrial applications. This work was carried out taking into consideration the results of a former work [1] to design a new experiment. The set of irradiated samples include GaAs and Ge homojunctions, GaInP/Ge double junctions and GaInP/GaAs/Ge triple junctions (TJ) solar cells. The experiment included in-situ dark and illuminated I-V curve measurements and modeling; ex-situ measurements were also performed, including external quantum efficiency and DLTS spectroscopy. In this paper, the preliminary studies of III-V solar cell damage using 10MeV proton irradiation are presented, so as some insight in the interpretation of results. Different characterization techniques and numerical simulation were applied to this objective.

## 2 EXPERIMENTAL SETUP

All experiments have been performed under high vacuum using a specially developed chamber installed in one of the experimental lines of the CNEA tandem accelerator (for further details see also Refs. [2],[3]). In order to spread the beam, a 10  $\mu\text{m}$ -thick aluminium foil was installed in the beam path about 6 m before the chamber (Fig. 1). The resulting beam intensity uniformity at the target position was determined before the

experiment by using an array of 9-Faraday cups (FC) positioned a few centimeters behind the sample holder. The beam current in each FC was measured using a Keithley 6514 electrometer.

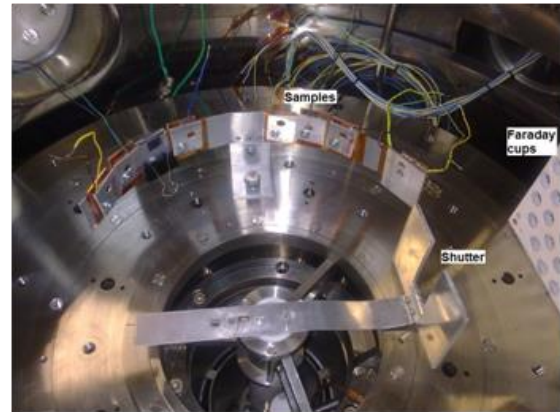


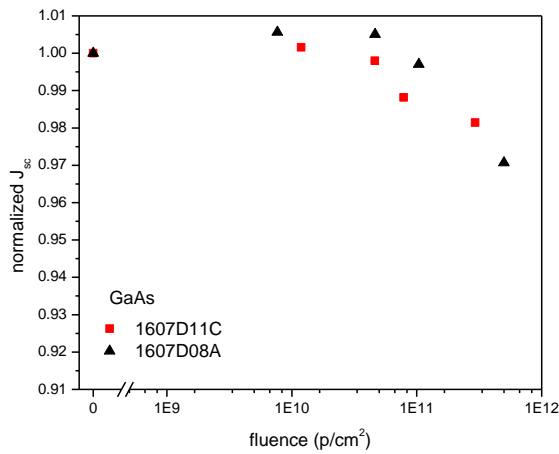
**Figure 1:** Top view of the irradiation chamber. The holder with the samples is on the upper side of the picture. All solar cells were wired to allow in situ measurement of I-V curves. The array of Faraday cups is seen at the right border of the picture.

The results of these measurements were recorded in a local computer and this information was replicated in a second computer sitting in the accelerator control room. The overall beam uniformity was better than 5% over the whole target area. To observe the evolution of the degradation of the devices during irradiation, the beam was interrupted at different fluence values, allowing the measurement of I-V curves at each step. The solar cells used in this study were fabricated employing the metalorganic vapor phase epitaxy (MOVPE) technique. The devices, with active areas of 1 mm<sup>2</sup>, were encapsulated on copper plates. The irradiated cells set included GaAs,

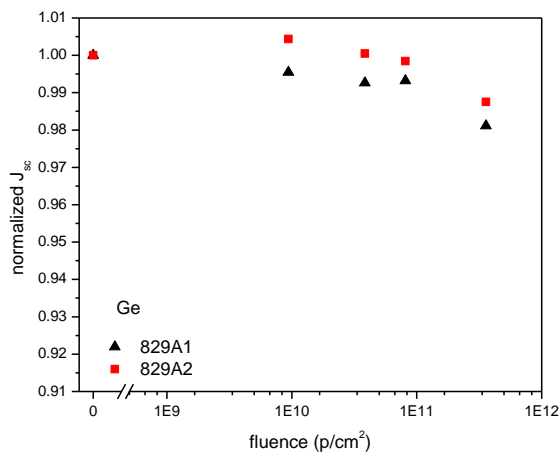
GaInP and Ge homojunctions, one GaInP/Ge double-junction and two GaInP/GaAs/Ge triple-junctions (TJ). The cells were measured ex situ before and after irradiation using a TS-Space AM0 close match solar simulator at  $T = 28^\circ\text{C}$  with  $1.367 \text{ kW/m}^2$  (equivalent to AM0 spectrum) calibrated with isotype and triple junction reference cells. In addition, the solar cells were measured in situ before and after each irradiation by a Sciencetech solar simulator with AM0 filter coupled to the irradiation chamber through a borosilicate window and a source measure unit (SMU) Keithley 2602A using the four wire configuration. All I-V curves are presented under standard conditions (1 sun AM0,  $28^\circ\text{C}$ ) after temperature and irradiance corrections using as reference the measurements performed with the TS-Space simulator.

### 3 EXPERIMENTAL RESULTS

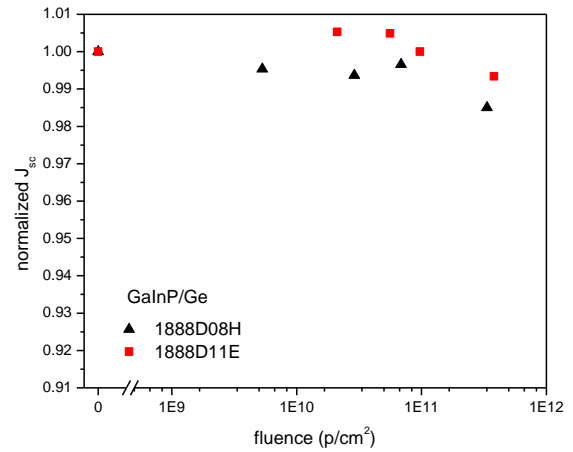
As example of the evolution of the cells electrical parameters versus fluence, Figure 2 shows the normalized  $J_{sc}$  degradation curves obtained for GaAs and Ge homojunctions, GaInP/Ge double-junction and GaInP/GaAs/Ge triple-junction.



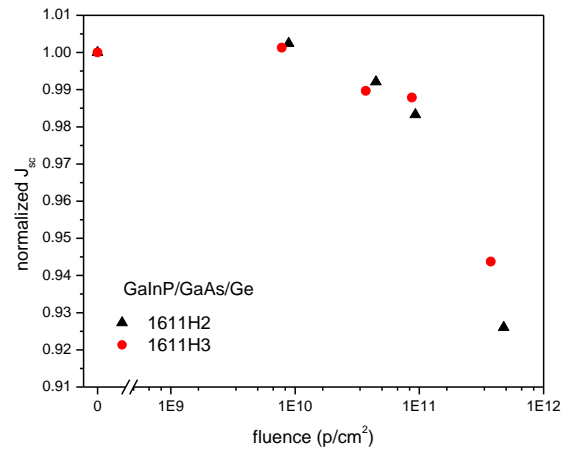
(a)



(b)



(c)



(d)

**Figure 2:** Normalized  $J_{sc}$  vs. fluence for: a) GaAs solar cells, b) Ge solar cells, c) GaInP/Ge double junction solar cells and d) GaInP/GaAs/Ge triple junction solar cells.

The degradation of the  $J_{sc}$  is the expected for this type of cells and these particular experimental conditions. GaInP cells showed the lower sensitivity to irradiation, while GaAs showed the higher. A minor trend to degradation, close to the experimental error, is also observed for the Ge cells. In the case of the TJ cells, the GaAs subcell (middle) degradation limits the overall current. In this context, current degradation was found quantitatively consistent when the spectral response of the middle cell (Fig. 3) was used to get the subcell current after irradiation.

The external quantum efficiency (EQE) was measured at IES-UPM before and after irradiation. Changes of EQE of the GaAs and the TJ solar cells are shown in Fig. 3. The curve of the GaAs cell drops in the wavelength range between 700 - 900 nm, consistently with the degradation of the diffusion length in the base of the device due to irradiation. Similar results are presented, for example, in references [4] for 10 MeV proton irradiation on a GaAs/Ge solar cell and [5] for a GaInP/GaAs/Ge TJ using 2.8 MeV protons.

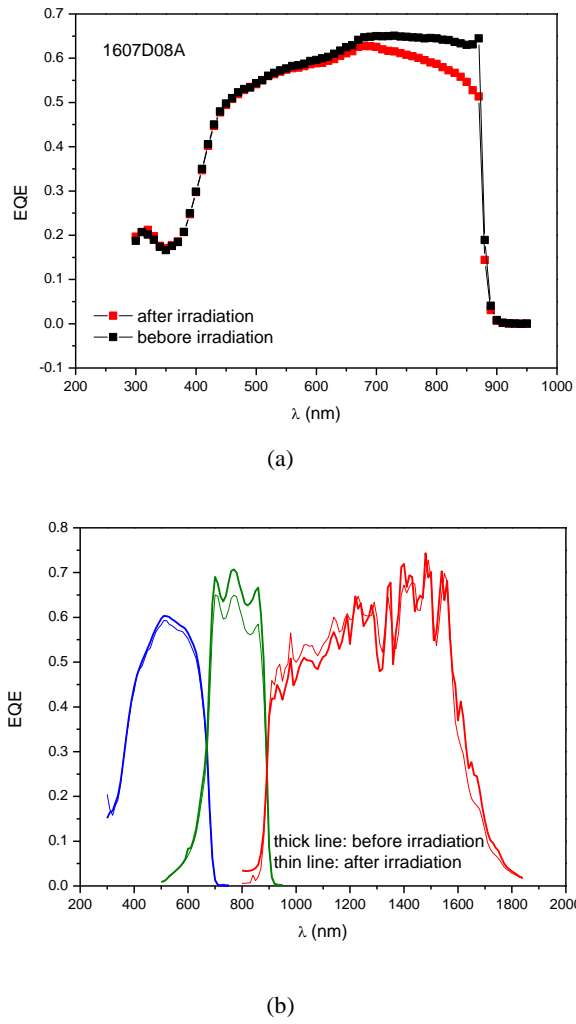


**Figure 3:** External Quantum Efficiency for: a) GaAs solar cells and b) GaInP/GaAs/Ge triple junction solar cells.

An interesting effect is observed in the Ge bottom cell, whose EQE seems to increase after proton irradiation. This effect suggests a quenching of the photon coupling

between the middle and bottom subcells after irradiation. In other words, before irradiation the measured EQE of the Ge bottom cell is artificially low (and shows some response from 800 nm to 900 nm) as a result of photon coupling from the GaAs middle cell. Once irradiated, the radiative recombination of the middle cell is greatly decreased and the real (higher) EQE of the bottom cell is measured.

#### 4 NUMERICAL SIMULATIONS

The electrical transport and light absorption in GaAs solar cells were studied with the computer code D-AMPS-1D [6]-[7]. D-AMPS is an updated version of the one-dimensional (1D) software AMPS (Analysis of Microelectronic and Photonic Devices) developed at The Pennsylvania State University, University Park, USA [8]. In AMPS finite differences and the Newton-Raphson technique are used to solve the system of the Poisson and continuity equations subjected to appropriate boundary conditions [9]. The three selected unknowns were the quasi-Fermi levels  $E_{FN}$  and  $E_{FP}$  and the electron potential  $\Psi$  [9]. Structures such as homojunctions, heterojunctions, multijunctions, etc, resulting from stacking layers of different materials can be studied by appropriately selecting characteristic parameters such as the gap energy, carrier mobilities, absorption coefficients, and doping concentrations among others. The letter D stands for new developments like the amphoteric state physics [10], the Pool-Frenkel effect [7], the Defect Pool model [11], direct and recombination tunnelling [12],[7], gap and doping continuous grading, light scattering at rough surfaces, light interference, etc. These improvements implemented in D-AMPS allowed a better interpretation of characterization results and design of solar cells containing amorphous, microcrystalline, and crystalline semiconductor layers. More recently, in order to properly model recombination of electron-hole pairs in direct gap materials and in heavily doped crystalline semiconductors the mechanisms of band-to-band (direct) and Auger recombination were also added to the already existing Shockley-Read-Hall formalism.

In order to simplify the modelling and first discussions the radiation induced lattice defects are modeled as traps with a single energy level. The main parameters used in the simulations are listed in Table I.

	Window	Emitter	Base	BSF	Buffer	Sustrate
material	GaInP	GaAs	GaAs	AlGaAs	GaAs	GaAs
$E_g$ (eV)	1.85	1.42	1.42	1.85	1.42	1.42
d (nm)	25	177	4833	150	1000	350000
$N_D$ (cm <sup>-3</sup> )	$1 \times 10^{18}$	$1 \times 10^{18}$	0	0	0	0
$N_A$ (cm <sup>-3</sup> )	0	0	$1 \times 10^{17}$	$2 \times 10^{18}$	$1 \times 10^{18}$	$1 \times 10^{19}$
$B_R$ (cm <sup>3</sup> s <sup>-1</sup> )	$1 \times 10^{-10}$	$7.2 \times 10^{-10}$	$7.2 \times 10^{-10}$	-	$7.2 \times 10^{-10}$	$7.2 \times 10^{-10}$
$\mu_n$ (cm <sup>2</sup> V <sup>-1</sup> s <sup>-1</sup> )	400	2051	2051	400	2051	2051
$\mu_p$ (cm <sup>2</sup> V <sup>-1</sup> s <sup>-1</sup> )	40	95	95	40	95	95

**Table I:** Typical parameters used in the numerical simulations of GaAs cell.  $E_g$ : the band gap, d: layer thickness,  $N_D$ : donor doping density,  $N_A$ : acceptor doping density,  $\beta_R$ : radiative recombination rate coefficient,  $\mu_n$ : electron mobility and  $\mu_p$ : hole mobility.

The capture cross section for electrons and holes in the base at the discrete donor level were assumed  $1 \times 10^{-13} \text{ cm}^2$  and  $1 \times 10^{-15} \text{ cm}^2$  respectively, considering capture cross sections published in the literature [13]. The  $J_{sc}$  as function of the donor-like trap energy and density obtained with the simulations are shown in Figure 4.

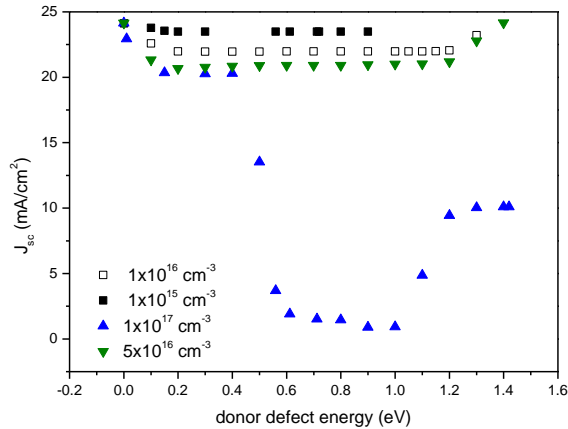


**Figure 4:**  $J_{sc}$  as function of the donor-like trap energy and density.

At the maximum defect density explored,  $1 \times 10^{17} \text{ cm}^{-3}$ , the short circuit current decreases to its minimum for trap energies near midgap. For a defect density of  $1 \times 10^{15} \text{ cm}^{-3}$   $J_{sc}$  decreases about 3% similarly to it is seen in Figure 2a for a fluence about of  $1 \times 10^{12} \text{ p/cm}^2$ .

Simulations performed with a discrete acceptor level showed no significant degradation considering similar capture cross sections as that used for the calculations showed in Fig. 4.

## 5 DLTS APPLICATION

We recently set up at DES-CNEA a DLTS (Deep Level Transient Spectroscopy) system based on a fast capacitor Boonton model 7200 with analogic output, a digitalizer DAQ National Instrument PCI-6132 S, and a pulse generator Agilent model 33220A. Sample temperature is controlled by a home made holder that includes a serpentine for LN2 circulation and a resistive heater, allowing temperatures between 80 K and 450 K using an electronic PID (Proportional-Integral-Derivative) commercial controller. The DLTS measurement is performed using a specially developed Labview code running in a PC.

Preliminary results obtained for a GaAs sample similar to those irradiated are shown in Fig. 5. Future measurements on irradiated samples will lead us to a better understanding of the effects of charged particle irradiation on solar cells.

By the other side, we studied the feasibility to describe the junction capacity transient using the analytical expressions developed by Z. Li [14], taking into account material properties, temperature, and the introduction of defect levels. This allowed us to perform numerical simulation of DLTS spectra.

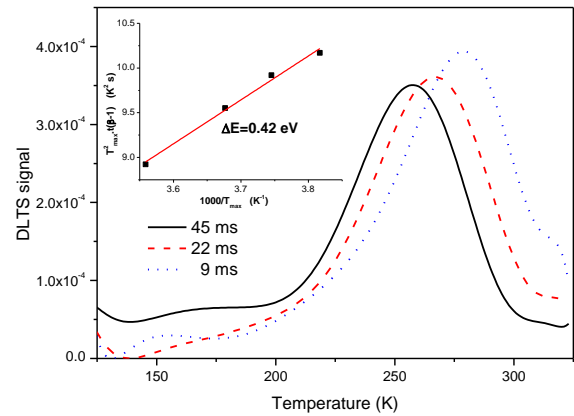


**Figure 5:** DLTS spectra for a GaAs device. Three rate windows were used; the corresponding Arrhenius plot is in the inset. The defect energy obtained is 0.42 eV (respect to the valence band).

## 6 CONCLUSIONS

A 10 MeV proton irradiation experiment was performed on III-V solar cells, and various characterization techniques were applied. This work was carried out taking into consideration the results of a former work to design a new experiment.

The results obtained show the expected trend of electrical parameters to degradation. Preliminary results of the numerical simulation of devices with D-AMPS- 1D code for single junction GaAs cells showed the feasibility of modeling the degradation of these cells introducing donor like defects in the gap.

In the future, experimental measurements of energy level and cross section of the defects will allow us to gain a better physical insight on the effects induced by the irradiation in III-V devices.

## 7 ACKNOWLEDGEMENTS

This work was funded by CNEA, the grants PIP2009-2011 N° 02318 and PIP2012-2014 N° 01052 (CONICET), PICT2007 N° 01143 and PICT2013 N° 3077 (ANPCyT), and the bilateral collaboration MINCYT-MICINN 2012-2013 (Argentina-Spain) N° ES/11/04 "Fabrication, characterization, simulation and test on solar cells based on III-V semiconductors".

## 8 REFERENCES

- [1] E. Yaccuzzi et al., In-situ and ex-situ characterization of III-V semiconductor materials and solar cells upon 10 MeV proton irradiation, Proceedings of the 28th European Photovoltaic Solar Energy Conference, 526 (2013).
- [2] M. Alurralde et al., Advances in the Development of Photovoltaics for Space Applications in Argentina, Proceedings of the 22nd European Photovoltaic Solar Energy Conference and Exhibition, 687 (2007).
- [3] M. Alurralde et al., Development of Solar Arrays for Argentine Satellite Missions, Aerospace Science and Technology **26**, 38 (2013).
- [4] W. Yueyuan et al., Radiation damage effects on double-junction GaInP₂/GaAs solar cells. Nuclear Instruments and Methods in Physics Research **B 330**, 76 (2014).
- [5] W. Rong et al., Effects of 0.28 - 2.80 MeV proton

- irradiation on GaInP/GaAs/Ge triple - junction solar cells for space use, Nuclear Instruments and Methods in Physics Research **B 266**, 745 (2008).
- [6] F.A. Rubinelli et al., Microcrystalline n-i-p tunnel junction in a-Si:H/a-SiH tandem cells, Journal of Applied Physics **89**, 44010 (2001).
  - [7] M. Vukadinovik et al., Transport in tunnelling recombination junctions, a combined computer simulation study, Journal of Applied Physics **96**, 7289 (2004).
  - [8] P.J. Mc Elheny et al., Range of validity of the surface-photovoltage diffusion length measurement: a computer simulation, Journal of Applied Physics **64**, 1254 (1988).
  - [9] F. Rubinelli et al., Computer modeling of solar cells structures, Proceeding of the 6th International. Photovoltaic Science and Engineering Conference, 811 (1992).
  - [10] F.A. Rubinelli and R.E.I. Schropp, Sensitivity of the a-Si:H based solar cell current-voltage characteristics to the adopted model for the density of states, Proceeding of the 2nd World Conference on Photovoltaic Energy Conversion, 998 (1998).
  - [11] E. Klimovsky et al., Characteristic curves of hydrogenated amorphous silicon based solar cells modeled with the defect pool model, Thin Solid Films **511**, 4826 (2007).
  - [12] F. Rubinelli, Direct tunneling at the front contact of amorphous silicon p-i-n devices, IEEE Transactions on Electron Devices **39**, 2584 (1992).
  - [13] J.C. Bourgoin and N. de Angelis, Radiation-induced defects in solar cell materials, Solar Energy Materials & Solar Cells **66**, 467 (2001).
  - [14] Z. Li, Systematic modelling and comparisons of capacitance and current based microscopic defect analysis techniques for measurements of high-resistivity silicon detectors after irradiation, Nuclear Instruments and Methods in Physics Research A **403**, 399 (1998).